PRAMANA
— journal of
physics

Vol. 61, No. 1
July 2003
pp. 167–176

Systematics of the $K^\pi = 2+$ gamma vibrational bands and odd–even staggering

J B GUPTA[1,2] and A K KAVATHEKAR[1]
[1]Ramjas College, University of Delhi, Delhi 110 007, India
[2]Address for Correspondence: 170/B-6, Sector 5, Rohini, Delhi 110 085, India
Email: j_b_gupta@hotmail.com

MS received 29 August 2001; revised 23 December 2002; accepted 23 January 2003

Abstract. The structure of the $K^\pi = 2+$ gamma vibrational bands and the quasi-gamma bands of even-Z–even-N nuclei is investigated on a global scale, vis-a-vis the variation of band head, the moment of inertia of the band and the odd–even spin staggering. The variation with N and Z and with spin J of the odd–even spin energy staggering index is studied and a unified view of the same is presented.

Keywords. Nuclear structure; staggering in gamma bands; medium mass nuclei.

PACS Nos 21.10.Re; 21.60.Ev; 27.70.+q

1. Introduction

The structure of low-lying $K^\pi = 2+$ gamma band in even Z–even N nuclei in $A = 130$–200 region has been studied by various workers [1–4] over the last four decades using various nuclear models. Whereas in the unified collective model of Bohr–Mottelson [1] it represents the axial symmetry breaking quadrupole vibration, in the rigid triaxial rotor (RTR) model of Davydov *et al* [2] it represents an anomalous rotation band. Wilets and Jean [3] used the γ-independent potential $V = V(\beta)$ for the collective structure, which yields a level pattern equivalent to the modified anharmonic oscillator, expressed as $E_{\lambda J} = \lambda(\lambda + 3)$, with J degeneracy. Here, the levels of γ-band are grouped as $2_2^+, (3_1^+, 4_2^+)\ldots$ as part of the λ-multiplets $2_1^+, (4_1^+, 2_2^+), (0_2^+, 3_1^+, 4_2^+, 6_1^+)$, in contrast to the RTR pattern of $(2_2^+, 3_1^+), (4_2^+, 5_1^+)$. It resembles the anharmonic vibrator split multiplets ($n = 2$ triplet: $4^+, 2^+, 0^+$, the $n = 3$ quintuplet: $6^+, 4^+, 3^+, 2^+, 0^+$), except that the 0^+ states are raised relative to the $J > 0$ member states.

In the group theoretical approach of the interacting boson model (sd IBM-1) [4], the band structure can belong to one of the three limiting symmetries of $U(6)$ algebra: viz. $U(5)$, $SU(3)$ and $O(6)$, corresponding to the anharmonic vibrator, deformed rotor and the γ-unstable W–J rotor respectively or a transition between them.

A host of workers [5–11] have studied in detail the odd–even staggering (OES) and the γ–g $B(E2)$ ratios in terms of these models. In [5], the ^{196}Pt and the $A \approx 130$ region were associated with the $O(6)$-like pattern and were reproduced in terms of the cubic d-boson interaction $(d^+d^+d^+)^{(3)}$ [9]. Zamfir and Casten [6] also used the OES index as a tool for the choice between the RTR and the $O(6)$ models. Peker and Hamilton [7] linked the odd–even staggering in the γ-band to the contribution of the Coriolis interaction besides the band interaction effects. Liao-Ji Zhi [8] illustrated the variation of the OES with angular momentum J of some well-deformed nuclei. Bonatsos illustrated the shift of odd-spin members from the even-spin ones in the γ-bands of Gd, Dy, Er and Yb [10] and attributed it to the β–γ band interaction. In their more recent work, Minkov *et al* [11] favored the γ–g band interaction as the main source of the OES. But their predictions of OES variation with spin J fell short of experiment.

We present the results of our global study of the band structure of $A = 130$–200 nuclei in terms of the Bohr–Mottelson model and the interacting boson model in a unified view and give a different perspective of the OES. In §2, firstly we discuss the general characteristics of the $K^\pi = 2+$ gamma band on a global scale and find its correlation to the g.s.-band and the $K^\pi = 0+\beta$ band. Section 3 deals with the variation of odd–even staggering with spin J and with N and Z. Finally in §4, we give the conclusion from this study.

2. The gamma band structure

2.1 *The band moment of inertia*

In an early review, Sheline [12] illustrated the link of the anharmonic vibrator level pattern and the g-, β-, and γ-vibrational band pattern of a deformed rotor. For the g.s.-bands, Mallmann [13] noted the correlation of the energy ratio $R_{6/2}$ (and of other $R_{J/2} = E(J)/E(2)$) with $R_{4/2}$, over the full range of $R_{4/2}$ values of 2.0 to 3.33, i.e., from the harmonic vibrator to rotor limit. Gupta *et al* [14] used the Mallmann plot to illustrate a smooth variation of these $R_{J/2}$ ratios as indicators of the smooth change in the intrinsic shape which affects the collective nuclear structure.

The smooth variation of g.s.-band level structure is reflected in the position and level pattern of the β- and γ-bands. For example, their moments of inertia are related to that of the ground state band. The plot of the β-band and γ-band moments of inertia $\theta_\beta = 3/[E(2_\beta) - E(0_\beta)]$ and $\theta_\gamma = 3/[E(3_\gamma) - E(2_\gamma)]$ vs. the g-band moment of inertia θ_g (figures 1 and 2) yields a diagonal relationship. Note that even for the shape transitional nuclei, the shape does not change significantly with (low) spin and low energy vibration, yielding equal moment of inertia of the three lower bands. Also, while θ_β exhibits significant deviations from the 45° diagonal, the γ-band moments of inertia θ_γ lie almost on the 45° diagonal and the scatter in data is rather small.

This difference between the γ- and β-vibration is also reflected in the variation of their band heads with neutron number N, across the major shell $N = 82$–126. While the β-band varies often sharply with N for a given Z value, the variation of the γ-band head is small and smooth (figure 3). At first 2_γ moves down with increasing valence neutrons up to the valley at $N = 90$ and rises thereafter.

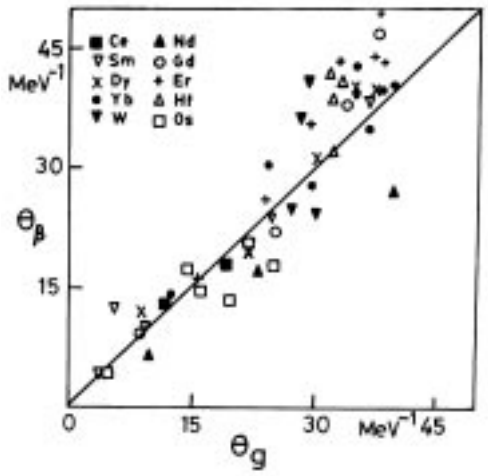

Figure 1. Moment of inertia of the β-band vs. the moment of inertia of the *g*-band.

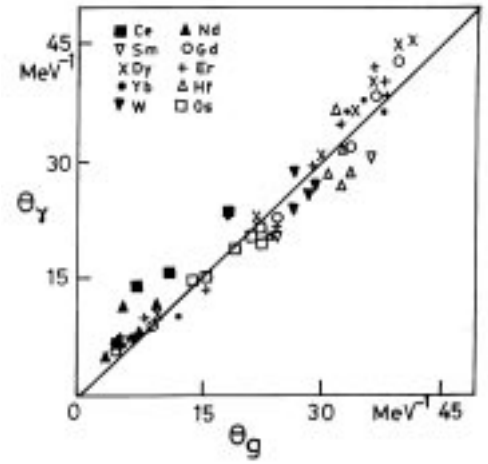

Figure 2. Moment of inertia of the γ-band vs. the moment of inertia of the *g*-band.

The smooth variation of θ_γ and of the γ-band head can be understood in terms of the intimate relation between the γ degree of freedom and rotation as reflected in the coupled eq. (1) of the rotation variables (θ, ϕ) and γ, as incorporated in the γ-part of the full β, γ separable equation [1,3]:

$$\Lambda\phi(\gamma,\theta_i) = \left[(-)\frac{1}{\sin 3\gamma}\frac{\partial}{\partial\gamma}\sin 3\gamma\frac{\partial}{\partial\gamma} + \frac{1}{4}\sum_{k=1}^{3}\frac{Q_i^2}{\sin^2(\gamma - 2k\pi/3)}\right]\phi(\gamma,\theta_i). \quad (1)$$

Here Λ is the separation parameter, the first term on the right signifies vibration with respect to the γ degree of freedom, and the second term represents the rotation. Since rotation

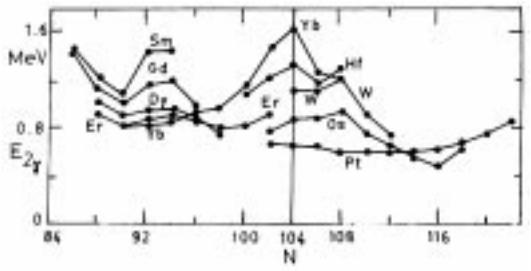

Figure 3. Plot of $E(2_\gamma)$ vs. neutron number N.

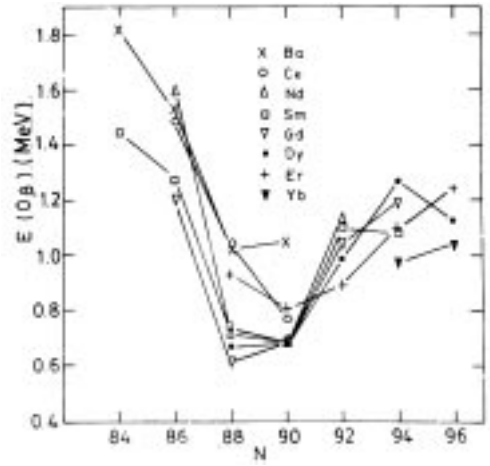

Figure 4. Plot of $E(0_\beta)$ vs. neuton number N.

depends on the nuclear core shape, which varies smoothly, the γ-band also varies smoothly. On the other hand the β-vibration is a dynamic effect.

However, the variation of $E(2_\gamma)$ is also partly dependent on the β-softness of the nuclear core and hence related to the position of 0_β in the shape transition region. For example, the valley at $N = 90$ is related to a similar valley for $E(0_\beta)$ at $N = 90$ (figure 4) (taken from [14]). The maxima of $E(2_\gamma)$ at $N = 104$ correspond to the β-hard core structure of these nuclei ($E(0_\beta)$ goes high when the nucleus is fully deformed). The inadequacy of the RTR model, which relates γ_0 to the ratio $E(2_\gamma)/E(2_g)$ (ignoring the β vibration, except through 2_g) is apparent.

2.2 *The energy spectra*

Next, consider the empirical energy formulae appropriate to the levels of γ-band. For $K > 0$, Bohr–Mottelson formula [1]:

$$E(J) = E_K + aX + bX^2 + cX^3 + \cdots + A_{2K}(-1)^{J+K} f(J), \tag{2}$$

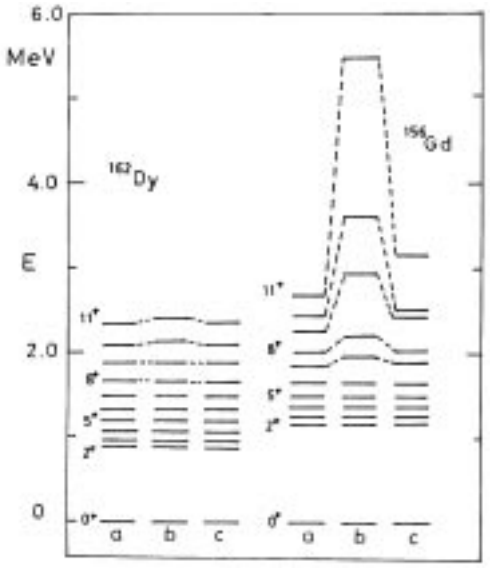

Figure 5. Energy fits of the γ-band levels in two typical nuclei (see text). Column (a) is for experiment and columns (b,c) for the values from eqs (2), (3) respectively.

where $X = J(J+1) - K^2$ and $f(J) = (K+J)!/(J-K)!$ was suggested. Application of eq. (2) to a very well-deformed nuclei gives a reasonable fit, e.g. up to $I^\pi = 11+$ in ^{162}Dy (figure 5) and ^{164}Er. But for other softer nuclei, say ^{156}Gd, eq. (2) fails badly (see column (b) in figure 5). Since large deviations occur on account of the steep increase in the values of successive terms in eq. (2) with J, an obvious remedy is to use a slower power series instead. Large improvement is obtained with power series in $X = [J(J+1) - K^2]^{1/2}$,

$$E(J) = E_K + aX + bX^2 + cX^3 + \cdots + A_{2K}(-1)^{J+K} f(J), \tag{3}$$

as is evident in column (c) for ^{156}Gd.

The OES term coefficient A_{2K} is always negative, except in a few cases (being very small positive), raising the odd spin level closer to the next higher even spin, as in the experiment. The variation with N of A_{2K} derived from eq. (3) is shown in figure 6. Its absolute value is large at the two ends of the major neutron shell but falls sharply as the number of valence neutrons or neutron holes increases, leading to increasing deformation of the core.

3. Odd–even staggering

3.1 *Variation with N and J*

The relative spacing of the odd–even spin levels in γ-bands differ from those of a deformed rotor, which is termed as the odd–even staggering (OES), as stated above. Casten and Brentano [5] noted the large OES for $A \approx 130$ isotopes of Xe and Ba $(N < 82)$ comparable to the broken $O(6)$ symmetry. The staggering index $S(J)$ defined as

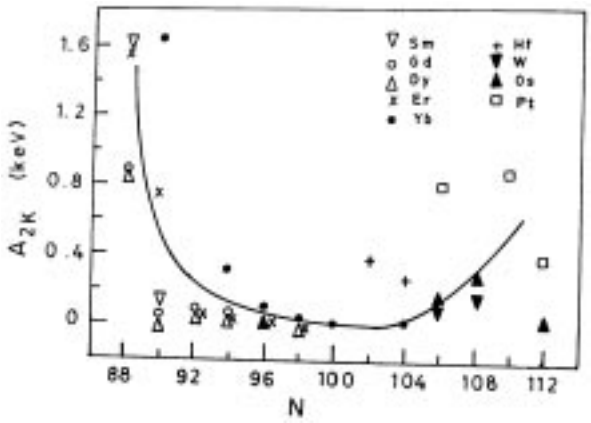

Figure 6. The variation of staggering coefficient A_{2K} (in eq. (3) by a fit to γ-band energies) with neutron number N.

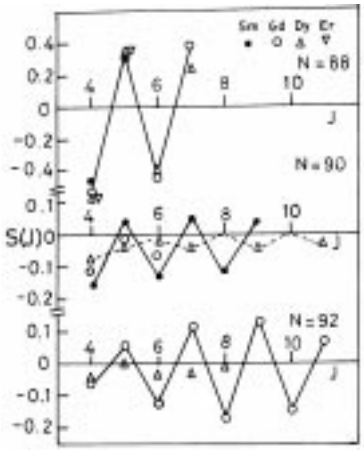

Figure 7. The staggering index $S(J)$ vs. J for various isotones.

$$S(J) = R(J)/(R(J)_{\text{adiabatic}} - 1, \tag{4}$$

with $R(J) = 2(E_J - E_{J-1})/(E_J - E_{J-2})$ was used to study the variation of staggering with J [15]. Using eq. (4) for $S(J)$ we plot $S(J)$ for $N = 88, 90, 92$ isotones separately (figure 7). Note the almost identical behavior of Sm, Gd, Dy, Er $N = 88$ isotones where $S(J)$ is almost constant with J (for both odd and even J), and is large $(S(J) = -0.5)$ compared to the limiting value of -1.0 (for even J) for anharmonic vibrator or γ-unstable rotor and $+0.27$ for the RTR model $(\gamma = 30^\circ)$. At $N = 90$, $|S(J)|$ is reduced to $\sim$15% of the γ-unstable rotor value for Sm, Gd and Dy, and decreases with increasing J. It also decreases with increasing Z. At $N = 92$, in Gd $|S(6)|$ is greater than $|S(4)|$ and is constant thereafter. In Dy $|S(J)|$ is much smaller. Much differing pattern is obtained in ^{162,164}Er (figure 8). In spite of the variations in the magnitude of $S(J)$, the sign of $S(J)$ (J = even) is always negative.

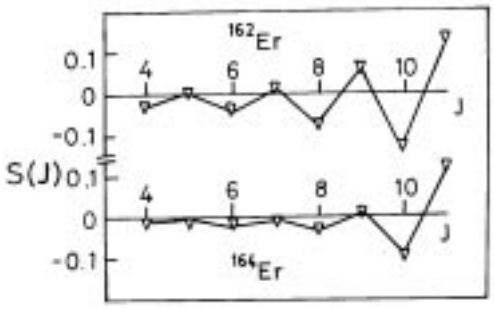

Figure 8. The staggering index $S(J)$ vs. J for ^{162,164}Er.

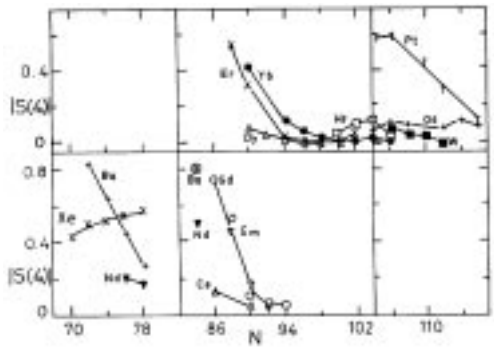

Figure 9. The staggering index $|S(4)|$ vs. N in half-shell quadrants.

3.2 *Variation with N in half-shell quadrants*

In view of the strong dependence of $S(J)$ on neutron number N we plot $|S(4)|$ vs. N, separate for each half major shell quadrants in view of the better picture in such a partition [16] (figure 9). In the first quadrant $(Z > 50, N > 82)$, $|S(4)|$ falls fast with increasing N for Nd, Sm and Gd. Similar behavior is seen for Er and Yb in the second quadrant $(Z > 66, N < 104)$, but the value of $|S(4)|$ stabilizes (to almost zero) for $N > 94$ as against $N = 90$ for Ce, Sm, Gd in quadrant I. This reflects the effect of larger Z in Er, Yb needing larger N for the same deformation and also corresponds to the different underlying Nilsson orbit patterns.

In quadrant III $(N \geq 104), |S(4)|$ is small for Yb, Hf, W and Os but is progressively larger for increasing Z. In terms of the IBM it is due to the decreasing number of hole bosons (N_p and N_n) and the resulting shape transition to γ-soft core. However, in Pt, $|S(4)|$ increases towards the mid-shell $N = 104$. In fact the lighter Pt isotopes get softened due to excess neutron holes and there is shape transition. Gupta *et al* [14] illustrated the sharp change in the g.s.-band level pattern in terms of the rotational coefficient exceeding the vibrational coefficient in the energy expression (E = sum of rotational energy and vibrational energy) for lighter Pt isotopes (see figure 6 in [14]). This affects the γ-band as well. The energy ratio $R_\gamma = E(2_\gamma)/E(2_g)$ is 2.3 in ^{188}Pt and jumps to 4.0 in ^{184}Pt, i.e.,

^{188}Pt is more triaxial. The $B(E2,0+ \rightarrow 2+)$ also exhibits the transition to larger values at $N = 106$ [14]. Bengtsson *et al* [17] noted a shift from oblate ground states above ^{188}Pt to more deformed prolate ground states in $^{182-186}$Pt.

In quadrant IV ($N < 82$) (see lower half of figure 7), the Ba and Xe isotopes exhibit opposite slopes of $|S(4)|$ with neutron number N. The slope for Xe is normal, i.e., $|S(4)|$ is larger for near $N = 82$ isotopes. The $B(E2,2_2 \rightarrow 0/2)$ ratio drops from 0.04 in ^{124}Xe to 0.006 in ^{130}Xe, which supports this change towards the $O(6)$ symmetry. In Ba, $|S(4)|$ increases from $N = 78$ towards $N = 72$ (as illustrated) and decreases for $N = 72$–66 ($|S(4)| = 0.60, 0.37$ and 0.46 for $N = 70, 68, 66$ respectively). In fact at $N = 72, 3_\gamma$ and 4_γ are almost degenerate, yielding the large $|S(4)|$. The 2_γ level is below 4_g in ^{132,134}Ba (as in RTR model) and overlaps with 4_g in ^{130}Ba. But these nuclei are not γ-rigid. Casten and Brentano [5] considered ^{134}Ba as the best example of $O(6)$ symmetry as also identified in ^{196}Pt. In both cases they illustrated the maximum triaxiality in terms of the greater cubic interaction term. Recently, ^{134}Ba is identified with $E(5)$ symmetry ($\beta > 0$, and γ-independent potential) [18,19].

The shape changes in Ba with N are exhibited through several variables. For example, the 0_β energy drops from 1.760 MeV in ^{134}Ba to 0.943 MeV in ^{128}Ba. For lighter isotopes 2_γ is above 4_g. The $B(E2,2_2 \rightarrow 0/2)$ ratio rises from 0.006 in ^{134}Ba to 0.092 in ^{128}Ba. Kumar and Gupta [20] in the study of light Ba isotopes in the microscopic approach have illustrated the potential energy surface (PES) of $^{122-134}$Ba exhibiting smooth transition from $N = 76$ to $N = 66$. The same is true for the quadrupole deformation β, the quadrupole moment $Q(2+)$, the $B(E2,2+ \rightarrow 0+)$. Thus the opposite slope for $N = 78$–72 represents the evolution from near closed shell ($N = 82$) pattern to the regular rotation–vibration structure.

3.3 *Variation with $R_{4/2}$ and N_pN_n*

A plot of $|S(4)|$ vs. the energy ratio $R_{4/2}$ illustrates the strong correlation of the odd–even staggering with the quadrupole deformation (figure 10). For $R_{4/2} < 2.7$ in the region of spherical or transitional nuclei, $|S(4)|$ drops from 0.75 to 0.2 smoothly with some scatter in the data. The Pt data have a different correlation as discussed earlier for the $|S(4)|$ vs. N plot. For $R_{4/2} = 2.7$–3.33, the region of soft deformed and well-deformed nuclei, $S(4)$ lies between 0.0 and -0.2. For individual isotopic chains also $|S(4)|$ falls with increasing $R_{4/2}$.

The product of valence nucleon pairs N_pN_n is a good measure of its effect in producing the deformation. This provides a link with the shell model. For $N_pN_n \geq 15$, on the average, the staggering index $|S(4)|$ falls with increasing N_pN_n (figure 11). For $N_pN_n > 30$, the nuclei are deformed and $|S(4)|$ is small (< 0.1). In the $N_pN_n = 3$–15 range, the data are more scattered and lie off the smooth curve. The $|S(4)|$ for Xe ($N < 82$) is falling with increasing N_pN_n but lie to the left of the smooth curve. The Ba $|S(4)|$ values for $N_pN_n = 6, 9, 12$ deviate from the smooth curve and rise with increasing N_pN_n. The Ba $|S(4)|$ values for $N_pN_n > 15$ ($N < 74$) do fall with increasing N_pN_n in agreement with the average trend. The same behavior is seen for Ce, Os and Pt. In general for N_p or $N_n \leq 4$, the nucleus is not deformed on account of the weak n–p interaction effects. Only when both numbers exceed 3 or 4, the deformation sets in and the OES index follows the regular trend.

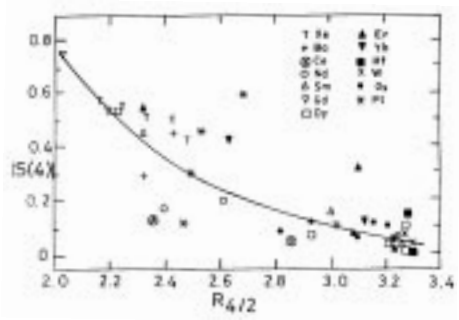

Figure 10. The staggering index $|S(4)|$ vs. $R_{4/2}$. The smooth curve is through the Gd data.

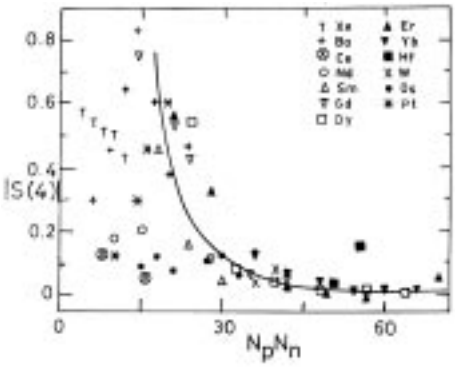

Figure 11. The variation of the staggering index $|S(4)|$ vs. N_pN_n. The smooth curve represents the general trend.

The scatter of $|S(4)|$ data in the preceding plot is larger than in the $|S(4)|$ vs. $R_{4/2}$ plot. This is due to the limitation of the shell model dependent N_pN_n product, which accounts only for the number of valence nucleons but not for single particle orbits which the nucleons occupy.

4. Conclusion

We have illustrated that, in general for low spins, the moment of inertia of β- and γ-bands vary equally with the ground-state band. The deviations are larger for $K^\pi = 0_2 + \beta$-band than for $K^\pi = 2+$ γ-band. There is little change in the quadrupole deformation of the core with rotation or vibration at low energy. Also for shape transitional nuclei, the level energies in the γ-bands vary with spin J as a geometric series in $X = [J(J+1) - K^2]^{1/2}$, including the OES term.

The sign of the odd–even energy staggering (OES) index in the γ-bands serves to distinguish between the rigid triaxial rotor shape and the γ-soft vibrator or the $O(6)$ symmetry. Its absolute magnitude indicates the degree of deviation from an axial rotor. The coefficient A_{2K} of the OES term in eq. (3) falls sharply towards the mid-shell. The OES index $S(4)$ in eq. (4) is large for the shape transitional nuclei and is much reduced for well-deformed

nuclei. The OES is related to the split multiplets of the anharmonic vibrator, wherein, the $3+, 4+$ states belong to the $n = 3$ quintuplet. Hence, these states lie closer as compared to the $2+$ state which belongs to the $n = 2$ phonon triplet. The same is true for the $(5+, 6+)$ and $(7+, 8+)$ in the higher n-phonon multiplets. This also explains the negative sign of $S(4)$ from eq. (4).

The Mallmann plots of $R_{J/2}$ vs. $R_{4/2}$ for the levels in the ground bands signify a smooth shape transition from spherical to well-deformed nuclei. Since $S(J)$ also represent shape effects, they too vary smoothly with $R_{4/2}$ or the product N_pN_n. The degeneracy breaking of the multiplet increases with increasing deformation, which ultimately changes to the rotational pattern. In a different language, this is treated in terms of the γ–g band mixing effects in soft deformed nuclei.

The different slope of $|S(4)|$ in figures 9–11 for Pt and Ba ($N = 78$–72) are due to the proximity of $N = 82$ closed shell. Near the closed shell, 2_2 is well below $4+$. As one moves away, the 2_2 state moves up and crosses $4+$, where $|S(4)|$ is maximum. Beyond this $|S(4)|$ decreases with increasing deformation. Thus independent of the detailed models, a unified view of the odd–even staggering in the gamma band is presented here (figures 6–11) in terms of the shape transition from spherical to deformed.

Acknowledgement

The financial support by University Grants Commission, Government of India is gratefully acknowledged.

References

[1] A Bohr and B R Mottelson, *Nuclear structure* (Benjamin, NY, 1975) vol. II
[2] A S Davydov and G F Fillipov, *Nucl. Phys.* **8**, 237 (1958)
[3] L Wilets and M Jean, *Phys. Rev.* **102**, 788 (1956)
[4] A Arima and F Iachello, *The interacting boson model* (1987)
[5] R F Casten and P von Brentano, *Phys. Lett.* **B152**, 22 (1985)
[6] N V Zamfir and R F Casten, *Phys. Lett.* **B260**, 265 (1985)
[7] L K Peker and J H Hamilton, *Phys. Rev.* **C16**, 486 (1977)
[8] Liao Ji-Zhi, *Phys. Rev.* **C51**, 141 (1995)
[9] K Heyde, *Phys. Rev.* **C29**, 1420 (1984)
[10] D Bonatsos, *Phys. Lett.* **B200**, 1 (1988)
[11] N Minkov, S B Drenska, P P Raychev, R P Roussev and D Bonatsos, *Phys. Rev.* **C61**, 064301 (2000)
[12] R K Sheline, *Rev. Mod. Phys.* **32**, 1 (1960)
[13] C Mallmann, *Phys. Rev. Lett.* **2**, 507 (1959)
[14] J B Gupta and A K Kavathekar, *Phys. Scr.* **56**, 574 (1997)
S Sharma, *Study of nuclear structure of some medium mass nuclei*, Ph.D. Thesis (University of Delhi, 1988)
[15] R F Casten, N V Zamfir, P von Brentano, F Seiffert and W Lieberz, *Phys. Lett.* **B265**, 9 (1991)
[16] J B Gupta, J H Hamilton and A V Ramayya, *Int. J. Mod. Phys.* **5**, 1155 (1990)
[17] R Bengtsson, J-Y Zhang, J H Hamilton and L K Peker, *J. Phys.* **G12**, L223 (1986)
[18] F Iachello, *Phys. Rev. Lett.* **85**, 3580 (2000)
[19] J M Arias, *Phys. Rev.* **C63**, 034308 (2001)
[20] K Kumar and J B Gupta, *Nucl. Phys.* **A694**, 199 (2001)